ENCLOSURE 7

STRUCTURAL INTEGRITY ASSOCIATES, INC.
REPORT 0900634.402, REVISION 2 (NON-PROPRIETARY)

UPDATED LEAK-BEFORE-BREAK (LBB) REPORT FOR PRAIRIE ISLAND NUCLEAR GENERATING PLANT UNIT 2 PRESSURIZER SURGE LINE NOZZLE

68 pages follow

Report No. 0900634.402
Revision: 2
Project No. 0900634
December 2009
☒ Q ☐ Non-Q

Updated Leak-Before-Break (LBB) Report for Prairie Island Nuclear Generating Plant Unit 2 Pressurizer Surge Line Nozzle

Prepared for:
Xcel Energy
(Contract No. 1006 Release 9)

Prepared by:

Structural Integrity Associates, Inc.
San Jose, California

Prepared by:	A. Chakraborty	Date: 12/18/2009
Reviewed by:	H.Qian	Date: 12/18/2009
Approved by:	G. A. Miessi	Date: 12/18/2009

REVISION CONTROL SHEET

Document Number: 0900634.402

Title: Updated Leak-Before-Break (LBB) Report for Prairie Island Nuclear Generating Plant Unit 2 Pressurizer Surge Line Nozzle

Client: Xcel Energy

SI Project Number: 0900634 ☒ Q ☐ Non-Q

Section	Pages	Revision	Date	Comments
All	All	0	12/07/2009	Initial Release
All	All	1	12/14/09	Client Comments Addressed.
All	1-2, 2-1 to 2-4, 3-3, 4-2 to 4-5, 4-7, 4-8, 4-11 to 4-14, 5-1, 6-1 to 6-5, 6-9, 7-1, 8-1, 8-2	2	12/18/09	Blacked out proprietary information. Also, changed references per client comments.

List of Tables

List of Figures

1.0 INTRODUCTION

A Leak-Before-Break (LBB) evaluation for the Unit 2 pressurizer surge line nozzle for the Prairie Island Nuclear Generating Plant was performed in accordance with 10 CFR 50, Appendix A, General Design Criterion 4 (GDC-4), "Environmental and Dynamic Effects Design Bases" [26] by Westinghouse as documented in Reference 1. The acceptable fracture mechanics procedures and criteria for LBB application are documented in NUREG-1061, Volume 3 [3] and subsequently incorporated in Standard Review Plan (SRP) 3.6.3 [2a]. However, in the existing LBB evaluation [1] the Alloy 82/182 weld connecting the carbon steel surge nozzle to the stainless steel safe end which is susceptible to primary water stress corrosion cracking (PWSCC) was not considered.

One of the limitations imposed by the NRC in SRP 3.6.3 and NUREG-1061, Vol.3 [3] is that locations on piping systems that are susceptible to corrosion mechanisms such as PWSCC do not qualify for application of LBB. In a more recent revision of SRP 3.6.3 [2b], it is stated that non-conforming piping that has been treated by two mitigation methods may qualify for LBB if the piping contains no flaws larger than those permitted by ASME Section XI [7] without repair.

Xcel Energy Corporation has performed weld overlay repair for the Alloy 82/182 dissimilar metal welds (DMW) at Prairie Island Unit 2 to mitigate PWSCC at these welds. A full structural weld overlay (FSWOL) has already been applied for the pressurizer surge line nozzle [31]. Reference 4 reports the required full structural weld overlay thicknesses for both the DMW and the neighboring stainless steel weld (SSW). The application of the overlay with Alloy 52M weld metal provides a PWSCC resistant barrier and also results in substantially reduced stresses on the inner portion of the configuration, thereby providing further protection against PWSCC initiation. Thus, the application of the weld overlay provides two mitigation methods in addition to providing a smooth surface that can enhance future non-destructive examination (NDE).

The calculated weld overlay thickness in Reference 4 is the minimum required for structural reinforcement. This full structural weld overlay thickness may be increased to account for fatigue crack growth, weld metal dilution, and machining allowance in the final overlay design.

Reference 5 reports both the minimum and maximum FSWOL designs. The application of the weld overlay changes the geometric configuration of the component and as such, the existing LBB evaluation reported in Reference 1 is being updated in the current report to reflect the new configuration utilizing the as-built WOL configuration as reported in Reference 31, whenever possible. Also, the thermal loads for new plant operating conditions for measurement uncertainty recapture (MUR) under power uprate (PU) will be considered. The objective of this report is to summarize evaluations of the LBB aspects of a weld overlay already installed at the Unit 2 pressurizer surge line nozzle at Prairie Island and to show that LBB margins are still maintained. The overall approach adopted in this report to show that the weld overlay locations on the Unit 2 pressurizer surge line nozzle at Prairie Island meet the requirements stipulated in SRP 3.6.3 and NUREG-1061, Vol. 3 is as follows:

- Review the methodology and margins in the existing LBB submittal (Section 2.0)
- Address the effectiveness of PWSCC mitigation by application of the weld overlay and demonstrate that the post weld overlay crack growth (both PWSCC and fatigue) are within acceptable limits for balance of plant life (Section 3.0).
- Describe the design input for the LBB evaluations (Section 4.0).
- Determine critical through-wall flaw sizes with the application of the weld overlay at the dissimilar metal welds (Section 5.0).
- Determine leakage through half the critical flaw sizes and show that the leakage is greater than the detectable leakage of 2 gpm (10 times the minimum plant leakage detection capability of 0.2 gpm per Section 5.2.3 of Reference 1). Alternately, show that the leakage flaw sizes for 2 gpm leakage are less than half critical flaw sizes. The PWSCC morphology for the existing nickel alloy welds will be considered in the determination of the leakage (Section 6.0).
- Provide conclusions of the evaluations (Section 7.0) and references used in the report (Section 8.0).

The technical approach utilized in this evaluation is consistent with the fracture mechanics methodology and criteria used in the original LBB report [1]. That technical approach is modified to deal with the addition of the weld overlay and the consideration of the PWSCC crack morphology along with the updated MUR loads for power uprate condition. However, the fundamental methodology, based on limit load and elastic-plastic fracture mechanics, and the LBB criteria remain unchanged.

2.0 SUMMARY OF EXISTING LBB EVALUATION

The application of LBB evaluation as a method for meeting the requirements of General Design Criteria 4 (GDC-4) was performed by Westinghouse [1]. At the time of the original evaluation, it was not recognized that the pressurizer surge line nozzle dissimilar welds were susceptible to PWSCC. Requirements in NUREG/CR1061, Vol. 3 [3], required that the use of LBB in areas where susceptible material is present would require mitigating measures and NRC review/ approval. SRP 3.6.3, Rev. 1 states that piping systems that are susceptible to active stress corrosion cracking mechanisms may qualify for application of LBB evaluation if treated with two mitigation methods and the piping contains no flaws larger than those permitted by ASME Section XI without repair.

The original LBB report considered bounding material properties and loads for the Unit 2 surge line. The surge line is connected to the Hot Leg surge nozzle at one end and to the pressurizer nozzle at the other end. The weld locations are considered critical for LBB evaluation. All the welds at Prairie Island Unit 2 surge line are fabricated using the gas tungsten arc weld (GTAW) and shielded metal arc weld (SMAW) procedures. Node 1320 (reducer to piping weld) was found to be the governing location where the stress levels and the weld procedures were both taken into account as bounding for all the locations of the Prairie Island Unit 2 pressurizer surge line.

Since thermal stratification can cause large stresses during heatup and cooldown, it was included in the Westinghouse LBB evaluation. For leakage evaluation, three load cases were considered, namely the normal operating condition (Case A), normal operating condition with stratification for temperature range from [redacted].

The critical flaw size calculation followed the same methodology. Four cases were developed (Case D through Case G in Table 4-2 of Reference 1) corresponding to the various stratification cases.

The leakage cases and critical flaw sizes cases were then combined to form six possible leak-before-break loading scenarios in the Westinghouse LBB report [1]. Out of the six possible scenarios, two governing loading combinations, Case B/G and Case B/F were found to be critical based on their margins, or ratio of critical flaw size to leakage flaw size for 2 gpm leakage (Table 7-1 of Reference 1).

[redacted]

[redacted], are reproduced in Table 3-1 of this report. Average material properties are used for leakage and minimum material properties are used for critical flaw size evaluations.

For the fracture mechanics evaluation, the weld was conservatively assumed to use the SMAW process, thus the Z factor was given as:

[redacted].

Ramberg-Osgood (R-O) parameters are not discussed or presented for the leakage evaluation; so, it is assumed that the crack opening displacement was only that due to the elastic response.

The margin, or ratio of critical flaw size to leakage flaw size, for both the events ([redacted]) were higher than the minimum requirement of 2, even for the extremely low probability event defined by Case B/G. Therefore, the LBB criteria were met easily.

Table 2-1. Material Properties at Surge Line Reducer to Piping Weld for Westinghouse LBB Evaluation

Temperature (°F)	Minimum Yield (psi)	Minimum Ultimate (psi)	Flow stress, average of Yield and Ultimate (psi)	Average Yield (psi)	Modulus of Elasticity, E (ksi)
[redacted]					

3.0 QUALIFICATION OF WELD OVERLAID PIPING FOR LBB

The technical basis for weld overlays is presented in MRP-169 [8]. The purpose of the MRP-169 report is to define methodology and criteria for the use of pre-emptive weld overlays (PWOLs) as a mitigation measure for PWSCC in PWR primary coolant pipe and nozzle welds. MRP-169 documents these criteria, and presents examples of their application. Key elements of MRP-169 are discussed in the following sections.

3.1 Thickness Considerations

In the application of a weld overlay in a plant, the weld overlay thickness may vary significantly. In addition to allowable tolerances, the overlay may be full structural (taking credit for none of the underlying base material) resulting in a relatively thick overlay or it may be optimized (taking credit for a portion of the underlying base material). For the evaluation presented for Prairie Island Unit 2 pressurizer surge line nozzle, a full structural weld overlay design is considered which has already been implemented. In the absence of as-built data, a range of thicknesses are considered between the minimum required for structural purposes to the maximum allowed as governed by inspection and other serviceability requirements as shown in the drawing in Reference 5. The WOL design thickness range is considered to show the bounding leakage results. For a given original pipe geometry, using the as-built weld overlay thickness (when available) will provide more accurate leakage result and the result will be bounded by the minimum required and maximum allowed thickness results, without a significant change in the conclusions related to LBB. It can be noted here that as-built dimensions for pipe and the weld overlay are used for the DMW as obtained from Reference 31.

The fundamental assumption of structural weld overlay sizing is that a crack is present in the original pipe or nozzle weld, which must be evaluated in accordance with ASME Section XI flaw evaluation rules [7, 9]. These rules establish an end-of-evaluation-period allowable flaw size based on the maximum size flaw that can be sustained in the component without violating original design margins (typically ASME Section III for primary system components).

A full structural weld overlay (FSWOL) is designed under the assumption that the base material is completely cracked. In the case of low applied loads at the overlay location, the ASME Section XI flaw depth limit of 75% of the wall thickness controls the weld overlay thickness (equivalent to one-third of the base metal thickness). In the case of higher applied loads, additional thickness may be required. Based on inspection requirements and the actual field application, the actual thickness may be somewhat greater.

Weld overlay sizing requirements are further defined in Code Cases N-504-3 and N-740-2 [10, 11] for FSWOLs. These overlays may be used for any application in which cracking has been detected in a weld consisting of a combination of a nozzle, pipe or safe-end. ASME Code Section XI allowable flaw size criteria (IWB-3640 and Appendix C) are used for sizing the weld overlay, based on the assumption that a circumferential crack is present, completely through-wall and 360° around the circumference of the original base material.

3.2 Mitigation of PWSCC Crack Initiation

The application of a weld overlay produced substantially reduced stresses [27] in the material beneath the weld overlay due to the shrinkage of the weld overlay material during its installation. A key aspect of the weld overlay design process is to demonstrate that favorable residual stress reversal occurs such that PWSCC initiation and growth is mitigated. Extensive analytical and experimental work was performed on weld-overlaid BWR pipe-to-pipe welds of various pipe sizes to demonstrate that favorable residual stresses result from full-structural weld overlays [12, 13]. A recent Pre-emptive Weld Overlay (PWOL) test program [8] also demonstrated that measured residual stresses in a typical PWR mid-sized DMW weld overlay were highly favorable when applied to a weld with a severe inside surface repair.

For application of weld overlays in PWR plants, a joint specific, overlay specific weld residual stress analysis is required for each unique PWOL configuration in which there is a significant geometry, material, or welding process difference from a previously analyzed overlay (beyond standard drawing/fabrication tolerances). These must be performed with analysis methods and tools that are appropriate for this type of analysis, including transient thermal analysis capability, non-linear elastic-plastic modeling capability, and temperature dependent material properties. Several such tools exist and have been demonstrated to produce residual stress results that are in agreement with (or conservatively bound) experimental measurements. The residual stress analysis considers actual welding parameters to be used in applying the weld overlay, including bead sequence, welding direction, heat input, thermal boundary conditions (wet or dry) and inter-pass temperature limits.

The initial residual stress condition of the DMW joint has a significant bearing on its susceptibility to PWSCC, especially as influenced by in-process repairs performed during plant construction. In fact, in essentially all cases in which PWSCC has been discovered in PWR butt welds, evidence of significant in-process repairs during construction has been found. Thus, to adequately demonstrate the favorable residual stress effects of a weld overlay, one must start with a highly unfavorable, pre-overlay residual stress condition such as that which would result from an ID surface weld repair during construction. If the nozzle-specific weld overlay design is shown to produce favorable residual stresses in this severe case, one can be assured that it will effectively mitigate against future PWSCC in the DMW.

Acceptable residual stresses for purposes of satisfying this requirement are those which, after application of the weld overlay, are substantially reduced on the inner portion of the weld, over the entire length of PWSCC susceptible material on the inside surface, at operating temperature, but prior to applying operating pressure and loads. After application of operating pressure and loads, the resulting stresses must be compressive or small enough to ensure a low probability of initiating new PWSCC cracks and to limit the potential of significant crack propagation in the weld.

The combination of residual stress and crack growth criteria, in conjunction with required post-overlay inspections, provides protection against initiating new PWSCC cracks after application of the weld overlay and/or propagation of pre-existing cracks that would violate the overlay design basis.

3.3 Crack Growth Considerations

Specific analyses are performed in Reference 6 for the Unit 2 pressurizer surge line nozzle dissimilar metal welds (DMW) at Prairie Island to determine the crack growth after the application of the full structural weld overlay. The minimum design geometry is considered for the crack growth evaluation. It is shown in [redacted] The minimum and maximum weld overlay thicknesses (taken from

Reference 5) considered in the following section for the present LBB evaluation bound the overlay thicknesses considered for the crack growth analysis by both higher and lower margins for both the DMW and SSW. The minimum as-built WOL thickness reported in Reference 31 is [redacted] which is larger than the minimum thickness reported in Reference 7 for crack growth analysis. Hence, the conclusions from the crack growth analysis remain valid. Therefore, the current LBB evaluation is both comprehensive and bounding.

3.4 Inspection Considerations

This section provides a general overview of the inspection requirements implementation of the weld overlay repairs.

Examination requirements for weld overlays involve two aspects. One is the type of examination and the other is the required interval. The requirements for the type of examinations for weld overlays are defined in ASME Code Case N-504-3 and N-740-2 [10, 11]. They are summarized in Figure 3-1.

These requirements are consistent with current PDI techniques [28] and were originally developed for weld overlay repairs of IGSCC in BWR stainless steel welds, where the initiating flaws are fully characterized with respect to length and depth. Since the full structural weld overlay design for these repairs assumes that the original flaw is through the original pipe wall, evaluation of the outer 25% of the original pipe wall along with the weld overlay is considered conservative for pre-service and subsequent inservice examinations, in that it provides some advance warning if the flaw were to unexpectedly propagate.

As an alternative to the above requirements, for cases in which current examination requirements are satisfied by inspecting the inner 1/3 of the original DMW from the ID of the nozzle, the utility may continue to perform such examinations, in lieu of the WOL examinations specified above. In such cases, the OD examination requirement is just the overlay itself, and is required only for the pre-service inspection performed after PWOL application.

Weld overlays examinations must conform to the rules in the ASME Code, Section XI for welds in piping that require the procedures, equipment, and personnel to be qualified by a performance demonstration in accordance with Appendix VIII, as amended in 10CFR50.55a [26]. Currently, the utilities use the PDI qualification process [28] to satisfy these requirements. Procedures, equipment, and personnel used for examination of preemptive weld overlays shall be qualified in accordance with these rules [20, 10, 11].

The inspection interval and sample size for IGSCC mitigating weld overlays in BWR weldments are defined in NUREG-0313 [29]. NUREG-0313 defines examination requirements in terms of the category of IGSCC susceptible weldment. The categories of weldments are based on 1) the IGSCC resistance of the materials in the original weldment, 2) whether or not stress improvement (or overlay) has been performed on the original weldment, 3) whether or not a post stress improvement UT examination has been performed, 4) the existence (or not) of cracking in the original weldment, and 5) the likelihood of undetected cracking in the original weldment prior to the application of the overlay. The categories range from A through G, with the higher letter categories requiring augmented inspection intervals and/or sample size. Category A is the lowest category, consisting of piping that has been replaced (or originally fabricated) with IGSCC resistant material.

Recently issued MRP Primary System Piping Butt Welds Inspection and Evaluation Guidelines (MRP-139) [30] utilize a similar classification scheme Specifically, in accordance with MRP-139, PWSCC susceptible weldments with no known cracks (based on examination) that have been reinforced by a full structural weld overlay made of PWSCC resistant material are designated Category B. PWSCC susceptible weldments that contain known cracks that have been repaired by a full structural weld overlay are designated Category F.

For PWOL applications, the absence of cracking in the original weldment, the structural reinforcement and resistant material supplied by the overlay, the residual stress improvement provided by the PWOL, and the requirement to do a PDI qualified examination immediately following application of the PWOL are deemed to be consistent with a low letter ranking (Category B) for either full structural or optimized structural overlays. Therefore the following requirements for subsequent inservice inspections shall be satisfied:

1. For PWSCC susceptible weldments for which an inservice inspection is performed in accordance with ASME Code, Section XI, Appendix VIII, Supplement 10 [20] immediately prior to application of the PWOL, and such inservice inspection demonstrates the weld to be absent of any flaws or crack-like indications, future ISI of the welds shall be performed in accordance with current ASME Section XI Code requirements. This requirement is consistent with MRP-139 Category B, except that it is independent of whether the PWOL is a full structural or optimized structural overlay.

2. For PWSCC susceptible weldments for which an inservice inspection in accordance with ASME Code, Section XI, Appendix VIII, Supplement 10 [20] is not performed immediately prior to application of the PWOL, or in which flaws or crack-like indications are detected, the weldment must be assumed to be cracked. In such cases, future inservice inspections shall be performed consistent with requirements for cracked, WOL-repaired weldments (MRP-139 Category F). After the weld overlay and initial post-overlay examination, such weldments shall be inspected once in the next 5 years. If no new indications are seen or if no growth of existing indications is observed in the examination volume, the inspection interval shall revert to the existing ASME Code program. (Note: the assumption is that weld overlay repairs applied to this category will be full structural, not optimized structural.)

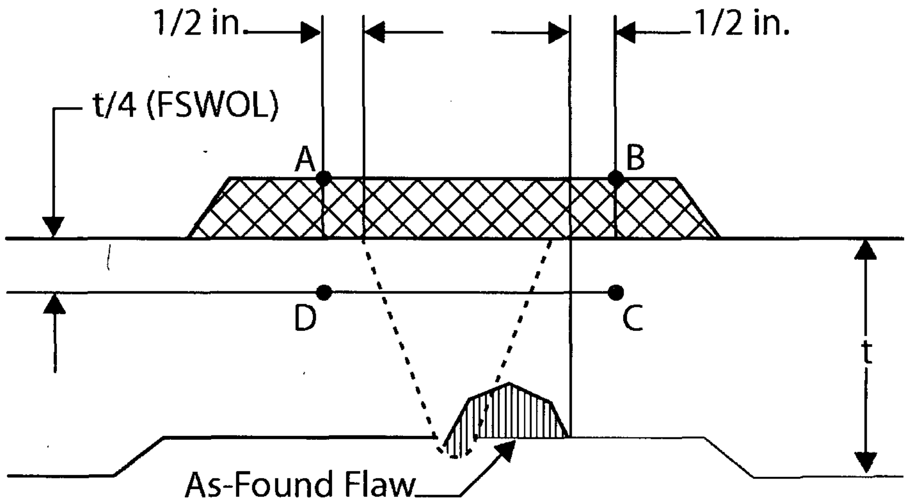

Preservice and Inservice Examination Volume A-B-C-D

Surface: Liquid penetrant examination of overlay material surface

Volumetric: Overlay directly over original PWSCC susceptible weldment (including nozzle, buttering, DMW and PWSCC susceptible safe-end if present) plus ½ inch beyond the as-found flaw and at least ½ inch beyond the toes of the original weld including weld-end butter, to a depth of the outer 25% of underlying material (A-B-C-D).

Figure 3-1. Preservice and Inservice Inspection Requirements for FSWOLs

4.0 LBB EVALUATION DESIGN INPUTS

4.1 Geometry

The weld overlay repair is applied on the DMW and the adjacent SSW on the Unit 2 pressurizer surge line nozzle. The material properties and geometry dimensions around the DMW and the adjacent SSW region have been changed while the rest of the surge line is not affected by the weld overlay application. The effect of PU conditions and revised whip restraint analysis loads applied on the entire surge line will be evaluated separately. However, only the DMW and the adjacent SSW locations with weld overlay repairs are evaluated for LBB in this report.

Figure 4-1 shows the schematic diagrams of the pressurizer surge nozzle weld overlay designs. In this evaluation, although only the DMW is susceptible to Primary Water Stress Corrosion Crack (PWSCC), the weld and base materials adjacent to it will be analyzed for completeness. Also for completeness, the SSW region will be analyzed too.

Four possible critical crack locations for the weld between the nozzle and the safe end (DMW) are (Figure 4-1(a)):

1. Nozzle near DMW
2. DMW Butter
3. Inside DMW
4. Safe end near DMW

Similarly for the SSW, the four possible critical crack locations for the weld between the safe end and the reducer are (Figure 4-1(b)):

1. Safe end near SSW
2. Inside SSW (near safe end)
3. Inside SSW (near reducer)
4. Reducer near SSW

These locations are designated as through-wall paths as shown in Figure 4-1. Evaluation of these locations will be performed to cover all the possible failure cases for the DMW and SSW.

For each overlay design, minimum required and maximum allowable weld overlay thicknesses will be evaluated. For the DMW, as-built thicknesses of base metal and WOL were measured at 4 points around the circumferential direction [31]. The maximum and minimum as-built WOL thicknesses are used in the critical flaw size calculation. Two different sets of maximum and minimum as-built WOL thicknesses are used from the 4 as-built measurements provided in Reference 31 for the critical flaw size and leakage calculations such that they give minimum critical flaw size and leakage for the corresponding configurations, respectively. Using the ID dimensions from Reference 5, the corresponding minimum and maximum ODs were calculated for Location 3. Hence, for each of the four postulated crack locations, two cases will be analyzed for each nozzle. The geometry data for each case is listed in Table 4-1 as obtained from References 5 and 31. It can be noted in Table 4-1 that some dimensions are different for critical flaw size and leakage calculations. This is due to the assumptions (i.e., considering cladding thickness only for leakage calculation) made to obtain both conservative critical flaw size (smaller thickness is more conservative) and leakage (larger thickness is more conservative) values.

4.2 Loads

The normal operating pressure for the weld overlay design is 2250 psia [14], or 2235 psig. Per communication with Prairie Island personnel, the normal operating pressure used is 1.01 times the original specified operating pressure [15], which results in a pressure of 2258 psig. Since higher pressure results in more conservative critical flaw sizes, and lower pressure results in more conservative leakage rates, 2258 psig is used in the critical flaw size calculations and 2235 psig is used in the leakage calculations. [redacted].

Per the guidance from SRP 3.6.3, the loads to be applied at the LBB critical locations are based on the algebraic sum of the normal operating loads (dead weight + thermal) for the leakage evaluation, and is based on the absolute sum of the normal operating loads and the Safe Shutdown Earthquake (SSE) loads for critical flaw size evaluation.

The thermal expansion and stratification loads are used in the evaluation are given in Table 4-2. All the values are entered as absolute values, to be consistent with the rest of the Table 4-2 from Reference 4. Thermal loads (TH) normally include only thermal expansion loads. For the pressurizer surge nozzle, however, since thermal stratification loads can be large, they are also considered. There are two kinds of thermal stratification loads: those occurring during normal operation and those occurring during heatup/cooldown transients. Thermal stratification loads during normal operation are combined with thermal expansion loads to form the thermal load, TH. Thermal stratification loads during heatup/cooldown are compared with SSE loads, and the higher of the two load types is used in the critical flaw size. The higher of the two is taken because simultaneous occurrence of SSE event during heatup/cooldown is highly unlikely.

Table 4-2 lists the pressurizer surge nozzle loads due to deadweight (DW) and SSE from Reference 4. The loads are applied to the safe end-to-reducer SSW in a global coordinate system with positive X axial parallel to the centerline of the nozzle [4]. The loads are then transferred to the nozzle-to-safe end DMW. The details of the calculations are included in the following sub-sections.

4.2.1 Design Loads for Critical Flaw Size Calculation at Safe End-to-Reducer Stainless Steel Weld

The thermal expansion loads using the pipe stress analysis are reported in Table 4-2. [redacted]. Since the higher axial load results in a lower thus more conservative critical flaw size, the axial load is taken as the absolute sum of the axial load from DW, TH and SSE.

Per SRP 3.6.3 [2], since all the moments are given as absolute values, for critical flaw size calculation, the total moments are calculated as square root of the sum of squares (SRSS) of moments from DW, TH, and SSE. The primary moment is given as the SRSS of DW and SSE. Since Reference 4 only specifies the axial direction, the non-torsional moments from Reference 4

(My, Mz of DW and SSE) cannot be added to the non-torsional moments from TH (denoted by Mx', Mz' of Thermal load) in Reference 4 directly. Therefore, to obtain the maximum moment possible, which results in a conservative critical flaw size, the resultant non-torsional moments from TH are assumed to be in the same direction as the resultant non-torsional moments from DW and SSE combined. Thus, the SRSS moment from Mx' and Mz' of TH was added to the SRSS moment of My and Mz from DW and SSE combined. Therefore, the total moment is calculated as the SRSS of the resultant non-torsional moments with the axial moment (My'+Mx) from TH, DW, and SSE combined as shown in Equation (1).

$$M_{total} = \sqrt{\left((M'_y)_{TH} + \Sigma_{\mathrm{DW},SSE} M_x\right)^2 + \left(\sqrt{(M_x')^2_{TH} + (M_z')^2_{TH}} + \sqrt{\left(\sum_{\mathrm{DW},SSE} M_y\right)^2 + \left(\Sigma_{\mathrm{DW},SSE} M_z\right)^2}\right)^2} \tag{1}$$

The primary moment (due to DW and SSE) is SRSS of the DW and SSE moments as shown in Equation (2).

$$M_{primary} = \sqrt{\left(\Sigma_{\mathrm{DW},SSE} M_x\right)^2 + \left(\sum_{\mathrm{DW},SSE} M_y\right)^2 + \left(\Sigma_{\mathrm{DW},SSE} M_z\right)^2} \tag{2}$$

The duration of the heatup/cooldown transients which causes the stratification loads is relatively short. Therefore, the corresponding stratification loads will not be combined with SSE loads as the combination with an extremely low probability. Hence, the higher of the stratification and SSE loads is considered. In this evaluation, the thermal stratification loads are lower than SSE load as shown in Table 4-2; thus, thermal stratification during heatup/cooldown is ignored in this LBB evaluation.

4.2.2 Calculated Loads for Critical Flaw Size Evaluation at Nozzle-to-Safe End Dissimilar Metal Weld

The loads from the safe-end-to-reducer weld (SSW) can be transferred to the nozzle-to-safe end weld (DMW) by the moment arm of [redacted] [4]. Note that a moment arm of [redacted] is used in weld overlay sizing calculation [4]. According to the overlay design drawing [5], [redacted]

[redacted] is the distance from the center of the SSW weld to the center of DMW weld and [redacted] is the distance from the center of SSW to the nozzle. Since the DMW is the area of interest in this LBB evaluation, [redacted] is used. Further study indicated that the moment arm[2] makes negligible difference in the final moment loads. Since all the forces and moments are reported as positive values and large moment yields conservative values for critical flaw size, the moments are transferred using Equations (3) through (5) for critical flaw size as follows:

$$Mx^* = Mx \tag{3}$$

$$My^* = My + Fz\,L \tag{4}$$

$$Mz^* = Mz + Fy\,L \tag{5}$$

The final loads used in the critical flaw size calculation are given in Table 4-3.

4.2.3 Design Loads for Leakage Calculation at Safe End-to-Reducer Stainless Steel Weld

For leakage calculations, axial forces are considered with their signs. The axial load for TH is positive [6]; the direction for axial load of DW is not available, thus assumed to be negative (axial load gives less leakage for a given crack size due to the tendency of the crack to close under such a force).

Since Reference 4 only specifies the axial direction, the non-torsional moments from DW may have different direction than moments from TH. Thus, a method to treat non-torsional moments similar to the one in Section 4.2.1 was developed. The difference is that, to obtain the minimum moment possible for leakage, the moments from TH are subtracted from DW as shown in Equation (6).

$$M_{total} = \sqrt{\left((M_y')_{TH} - (M_x)_{DW}\right)^2 + \left(\sqrt{(M_x')^2_{TH} + (M_z')^2_{TH}} - \sqrt{(M_y)^2_{DW} + (M_z)^2_{DW}}\right)^2} \tag{6}$$

4.2.4 *Calculated Loads for Leakage Calculation at Nozzle-to-Safe End Dissimilar Metal Weld*

The moments are transferred from safe end-to-reducer weld to nozzle-to-safe end weld using Equations (7) through (9). Note that all the "±" combinations in Equations (8) and (9) are utilized to obtain the minimum moments. The final loads used in the leakage evaluation are given in Table 4-3.

$$Mx^* = Mx \tag{7}$$

$$My^* = My \pm Fz \ L \tag{8}$$

$$Mz^* = Mz \ \pm Fy\, L \tag{9}$$

4.3 MUR Power Uprate Loads

Table 4-2a of Reference 18 showed that the maximum temperature difference from the heatup/cooldown transient is 304°F. Under MUR power uprate conditions, of all the transients that got affected by MUR, the maximum temperature difference is 246.8°F during a "Reactor Trip, Cooldown, & SI" Transient, [CN-PAFM-07-109_transients, containing Table 6.3-1 of Reference 18]. Since the stratification loads are proportional to the temperature difference, the thermal stratification loads based on heatup/cooldown transient will still bound the current MUR condition.

4.4 Material Properties

Material properties are taken from the ASME Code, Section II [19], and are checked for consistency with one of the weld overlay sizing calculations [4]. The mechanical strength for normal operating temperature is shown in Table 4-4. The modulus of elasticity is obtained from the ASME Code [19], and interpolated to the operating temperature with values shown in Table 4-4.

4.4.1 Z-Factors for Fracture Mechanics Analysis

For the pressurizer surge nozzle, since it is carbon steel, per ASME Code, Section XI, Appendix C [20], the Z-factors for ferritic/carbon steel base metals and associated weld metals are also calculated as follows:

For Seamless/Welded Wrought Carbon Steel pipe and pipe fitting with $\sigma_y < 40$ ksi and for welds made using carbon steel electrodes, the Z-factor is calculated as follows:

$$Z = 1.20[1+0.021A(NPS-4)] \tag{10}$$

For carbon and alloy steel (including SAW and SMAW welds) with $\sigma_y > 40$ ksi and Tensile Strength less than 80 ksi, the Z-factor is calculated as follows:

$$Z = 1.35[1+0.0184A(NPS-4)] \tag{11}$$

where:

$A = [0.125(R/t) - 0.25]^{0.25}$ for $5 \leq R/t \leq 10$

$A = [0.4(R/t) - 3.0]^{0.25}$ for $10 \leq R/t \leq 20$

R = mean radius, in.

t = thickness, in.

NPS = nominal pipe size

From Table 4-1, since $\sigma_y < 40$ ksi for the nozzle, Equation (10) applies. Using [redacted] Assuming $5 \leq R/t \leq 10$ still applies; the Z-factor for the nozzle is calculated as [redacted]

The weld material between the nozzle and the safe end is Alloy 82/182 (Alloy 600). A Pressure Vessels and Piping (PVP) conference paper [21] described analyses to determine the Z-factor for this material as

$$Z = 0.00065D^3 - 0.01386D^2 + 0.1034D + 0.902 \quad \text{for } D \leq 8'' \qquad (12)$$

$$Z = 0.0000022D^3 - 0.0002D^2 + 0.0064D + 1.1355 \quad \text{for } D \geq 8'' \qquad (13)$$

where:

D = the nominal pipe diameter, in.

Using [redacted], and Equation (13), [redacted].

The overlay is identified as a GTAW weld. For Alloy 52M, the Z-factor is 1 per ASME Code, Section XI, Appendix C [20].

The safe end material is stainless steel; the Z-factor is 1 per ASME Code, Section XI, Appendix C [20].

The reducer is made of austenitic stainless steel. Per ASME Code, Section XI, Appendix C [20], Section C-6330, the Z-factor for austenitic weld materials fabricated using shielded metal arc (SMAW) or submerged arc (SAW) welding is calculated as

$$Z = 1.30[1 + 0.010(NPS - 4)] \quad \text{for SMAW and SAW} \qquad (14)$$

where:

NPS = nominal pipe size, in; NPS is taken as the outside diameter of the component.

For conservatism, the Z-factor for the SAW (Equation 14) is applied for the austenitic stainless steel. Using [redacted].

Similarly, the Z factor for the stainless steel weld is conservatively assumed to be for SAW (Equation 14) and calculated as [redacted]. Z factors for all the materials are shown in Table 4-4.

4.4.2 Ramberg Osgood Parameters Based on ASME Code Minimum Values

The Ramberg-Osgood (R-O) relationship is used in elastic-plastic fracture mechanics analysis and in the leakage analysis to describe the stress-strain curve. Appendix C describes the R-O stress strain representation and describes how it may be determined using ASME Code minimum properties. The parameters α and n are determined using the methodology from Reference 22 as described in Appendix C. The Ramberg-Osgood parameters are presented in Table 4-5 for all the materials under consideration.

Table 4-1. Geometry[1]

		Nozzle to Safe End (DMW)					Safe End to Nozzle (SSW)			
Location		1	2	3(min)[4]	3(max)[5]	4	1	2	3	4
Base Metal	D_o, in	[redacted]								
	D_i, in									
	Thickness, in									
WOL (thickness)	Min., in									
	Max., in									

Notes: 1. Geometry data are taken from design drawing of WOL per Reference 5 except for Location 3 of DMW.

2. ID is taken from design drawing of WOL per Reference 5.

3. As-built thicknesses of base metal and WOL are used for Location 3 of DMW per Reference 31. OD is calculated from ID and the as-built thickness.

4. Using minimum as-built WOL thickness.

5. Using maximum s-built WOL thickness.

6. Numbers in brackets indicated geometry data used for leakage calculations, if different from the critical flaw size calculations.

7. Dimension include cladding thickness.

Table 4-2. Loads at Safe End-to-Reducer Weld for Critical Flaw Size evaluation

Condition	Force - Kips	Moments - in-kips		
	Fx	Mx	My	Mz
DW	[redacted]			
SSE				
	Fy'	My'	Mx'	Mz'
STRATIFICATION (127°F) [1]	1.37	429.90	143.06	180.07
STRATIFICATION (60.4°F) [2]	1.91	649.18	177.47	165.54
THERMAL EXPANSION (w/o restraint)	1.94	656.57	314.77	122.02

Notes: 1. The 127°F stratification corresponds to thermal stratification during heatup/cooldown transients.

2. The 60.4°F stratification corresponds to thermal stratification during normal operating conditions.

Table 4-3. Loads at Weld Locations

		Location	
		Safe End-to-Reducer Weld	Nozzle-to-Safe End Weld
Leakage Calculation	Axial Forces (Normal), kips	-6.15	-6.15
	Moment (Normal), in-kips	1321.6	1311.3
Critical Flaw Size Calculation	Axial Forces (Normal + SSE), kips	33.85	33.85
	Moment (Normal + SSE), in-kips	4837.3	5012.2
	Moment (DW + SSE), in-kips	3861.3	3996.4

Note: Normal Operation= Deadweight (DW) + Thermal (TH).

Table 4-4. ASME Code Strength for Pressurizer Surge line nozzle at Normal Operating Temperature [redacted]

Component/Material	Materials Designation [redacted]	S_y (ksi)	S_u (ksi)	σ_{flow} (ksi)	Modulus of Elasticity (ksi)	Z factor
[redacted]	Carbon Steel	29.54	70	49.77	26,064	1.39
	SB-166 (N06600) Bar, Annealed	29.68	80	54.84	28,435	1.19
	SB 166 (N06690) Bar/Rod	27.50	79.99	53.74	27,835	1
	Stainless Steel	15.28	61.59	38.44	25,035	1
	Austenitic Stainless Steel	18.48	71.80	45.14	25,035	1.44
	Austenitic Stainless Steel	18.48	71.80	45.14	25,035	1.44

Note: Flow stress is average of yield and ultimate tensile strengths for LBB evaluation

Table 4-5. Ramberg-Osgood Parameters for Pressurizer Surge Nozzle at Normal Operating Temperature ([redacted])

Component/Material	Materials Designation [redacted]	Ramberg Osgood Parameter α	Ramberg Osgood Exponent n
[redacted]	Carbon Steel	1.765	4.322
	SB-166 (N06600) Bar, Annealed	1.916	3.882
	SB 166 (N06690) Bar/Rod	2.024	3.659
	Stainless Steel	3.276	2.938
	Austenitic Stainless Steel	2.709	2.995
	Stainless Steel Type 308	2.709	2.995

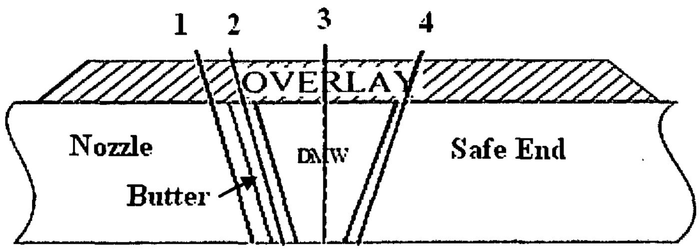

(a) Nozzle-to-Safe End Weld[a]

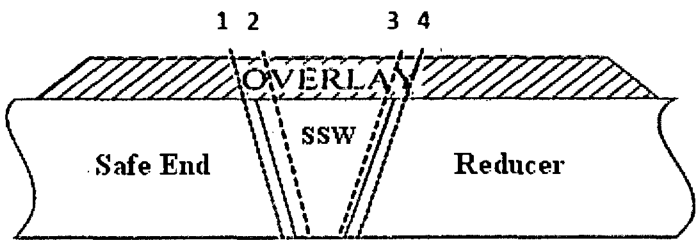

(b) Safe End-to-Reducer Weld[b]

Figure 4-1. Schematic Diagrams of Pressurizer Surge Line nozzle Weld Overlay Design

Notes:

(a) Postulated crack locations:

1. Nozzle near DMW
2. DM Weld Butter
3. Inside DMW
4. Safe end near DMW

(b) Postulated crack locations:

1. Safe end near SSW
2. Inside SSW (near safe end)
3. Inside SSW (near reducer)
4. Reducer near SSW

5.0 CRITICAL FLAW SIZE EVALUATION

5.1 Methodology

The LBB evaluation is performed for the Prairie Island Unit 2 pressurizer surge line nozzle DMW and the adjacent SSW. The limit load methodology described in Appendix A will be used to determine the critical flaw size. This is consistent with the approach provided in SRP 3.6.3 for limit load evaluation except that it considers the combination of geometry and material properties for a section with two different materials. For consideration of crack locations with low toughness material, Z-factors are used, consistent with the methods currently implemented in ASME Section XI for evaluation of piping and associated weldments.

5.2 Critical Flaw Size Determination

Critical flaw sizes were determined using the methodology of Appendix A, assuming the crack length was the same for the weld overlay and the underlying base material, consistent with the assumption of a constant length through-wall crack in SRP 3.6.3 [2(b)]. The critical flaw sizes are calculated for the weld overlay designs. Table 5-1 shows the resulting critical crack lengths for the DMW (Table 5-1(a)) and SSW (Table 5-1(b)), respectively.

5.3 Critical Flaw Size Comparison to the Original LBB Evaluation

Two test cases are also run to check the compatibility of the current methodology in this report with respect to the one in the critical flaw size evaluation from the original LBB report [1]. The parameters used for the test cases ('G' and 'F'), such as geometry, material properties, and loads are given in Section 2. The critical flaw sizes for G and F cases are 10.08 inches and 10.61 inches, respectively employing the methodology described in appendix A. The critical flaw length from Reference 1 for [redacted], respectively. Hence, the present evaluation produces approximately 14% smaller critical flaw sizes. The difference in critical flaw length values is due to the differences in the load calculations. The present calculation uses the outside radius to obtain the axial stress due to pressure whereas Reference 1 uses the inside radius.

Table 5-1. Critical Flaw Size Results

(a) Nozzle-to-Safe End Weld (DMW)

Path	Critical Flaw Size (in)	
	Min. WOL Design	Max. WOL Design
1	17.80	19.51
2	17.75	19.46
3	21.64	21.83
4	19.32	20.85

(b) Safe End-to-Reducer Weld (SSW)

Path	Critical Flaw Size (in)	
	Min. WOL Design	Max. WOL Design
1	18.40	19.89
2	17.04	18.70
3	16.06	17.83
4	16.06	17.83

6.0 LEAKAGE EVALUATION

6.1 Methodology

The leakage for ½ critical flaw sizes was evaluated using the PICEP [23] computer program. Since PICEP will only evaluate a single material, equivalent material properties are derived to use with PICEP. The total weld overlay thickness is used in the model for purpose of computing the leakage rate, along with a methodology to evaluate crack morphology as described in Appendix B.

6.2 Leakage Rate Calculations

The following summarizes the assumptions and design input used for the current leakage analyses:

1. Per the guidance in SRP 3.6.3 [2(b)], the loads to be applied at the LBB locations for the leakage evaluation are based on the algebraic sum of the normal operating forces and moments (Dead Weight + Thermal loads).

2. The LBB evaluation will be provided for the pressurizer surge line nozzle locations with Alloy 600 DMW and SSW with weld overlays. For these locations, the adjacent materials will also be considered as possible locations for a through wall crack. For the DMW, the adjacent materials are that of the nozzle and safe end, and that of safe end and reducer steel pipe for the stainless steel weld. The schematic of the regions of the DM and SS weld regions are shown in Figure 4-1.

3. The leakage analysis will be based on the nominal normal operating pressure of 2249.7psia (or 2235 psig) and the normal operating temperature of [redacted] as reported in Section 4.2. The material properties (as shown in Tables 4-4 and 4-5) are all based on [redacted].

4. PICEP options are assumed as follows:
    a. The option for combining axial forces and moments is used.
    b. A plastic zone correction is included. This is consistent with fracture mechanics principles for ductile materials.

c. The crack is assumed to be elliptical in shape with the inlet area equal to the exit area.
d. Crack roughness is taken as 0.000197 inches (5 micrometers) for fatigue cracks [24] in materials other than the Alloy 600 weld for which the value is given in Input 10. There are no turning losses assumed for fatigue cracking.
e. A sharp-edged entrance loss factor of 0.61 is used (PICEP default).
f. The default friction factor equations of PICEP are utilized.

5. Figure 4-1 shows the different postulated crack locations on the pressurizer surge nozzle that are considered for the leakage evaluations. Materials adjacent to the DM weld, although not susceptible to PWSCC, will be analyzed for completeness. For the DM weld, the postulated cracks are located as follows:

    1. Nozzle near DMW
    2. DMW Butter
    3. Inside DMW
    4. Safe end near DMW

   Similarly for SSW, the postulated cracks are located as follows:

    1. Safe end near SSW
    2. Inside SSW (near safe end)
    3. Inside SSW (near reducer)
    4. Reducer near SSW

6. For the pressurizer surge nozzle, cracks at 4 different sections are analyzed for both the DM weld and SS weld, (as shown on Figure 4-1). Minimum required and maximum allowable weld overlay thicknesses will be evaluated. The geometry data for each case is listed in Table 4-1. Specifically, as-built thicknesses of base metal and WOL were measured for the DMW at 4 points around the circumferential direction [31]. The maximum and minimum as-built WOL thicknesses are used in leakage calculation. Two (maximum and minimum) as-built WOL thicknesses are used from the 4 as-built measurements provided in the leakage calculation such that they give minimum leakage for a given flaw size for the corresponding configurations. Using the ID geometry from Reference 5, the corresponding maximum and minimum ODs were calculated for Location 3 in Figure 4-1 (a). It can be noted that, for conservatism, the pipe cladding, where present, is added to the base metal thickness values, but using the base material property.

7. Loads for the leakage calculation are given in Table 4-3.

8. The welds and base materials used in this evaluation are as follows:

   <u>Surge Nozzle:</u> [redacted]

Butter:

DM Weld:

Safe End:

SS Weld :

Overlay:
Reducer:

[redacted]

The material properties per ASME Code, Section II [19] are reported in Table 4-4. The Ramberg-Osgood parameters derived from the ASME Code minimum properties and are Table 4-5.

9. To determine material properties for the leakage evaluations with PICEP, composite material properties will be used based upon the relative thicknesses of the base material and the weld overlay. For example, for the yield stress, we have

$$S_{y_{Composite}} = \frac{\left(t_{base} \times S_{y_{base}} + t_{WOL} \times S_{y_{WOL}}\right)}{\left(t_{base} + t_{WOL}\right)}$$

This applies to modulus of elasticity, yield strength, and Ramberg/Osgood parameters.

10. For the weld with Alloy 600 (82/182), SCC susceptible material, the adverse effects of PWSCC crack morphology will be considered for the affected material. The assumed PWSCC crack morphology is for a crack parallel to the long direction of the dendritic grains. Below are the PWSCC crack morphology parameters as described in Reference 25:

μ_L	=	0.000663778 in
μ_G	=	0.0044842 in
N_{90}	=	150.87
L_G/t	=	1.009
L/t	=	1.243

where,

μ_L	=	Local roughness, inches
μ_G	=	Global roughness, inches
N_{90}	=	Number of 90 degree turns per inch
L_G/t	=	Global flow path length to thickness ratio
L/t	=	Global plus local flow path length to thickness ratio

11. For non-susceptible materials (i.e., Alloy 52M used as weld overlay), the crack morphology for air fatigue cracking is used. Below are the fatigue crack morphology parameters as described in Reference 24:

μ_L	=	0.000197 in
μ_G	=	0.000197 in
N_{90}	=	0
L_G/t	=	1.000
L/t	=	1.000

6.3 Results

Leakage flaw sizes were calculated based on a combination of PWSCC and fatigue crack morphologies for the Alloy 82/182 DM welds. For the non-susceptible metals, only the fatigue crack morphology was used. The leakage flaw sizes, which result in 2 gpm leakage for each of the postulated flaw paths, are calculated and shown in Table 6-1 for the DMW and SSW. In addition, the leakage rate through the calculated half critical flaw sizes are also determined and presented in Table 6-2 for the DMW and SSW. The leakage values are 2 gpm or higher.

Comparing the critical flaw sizes in Tables 5-1(a) and 5-1(b) and 2 gpm leakage flaw sizes in Tables 6-1, the flaw size margin between the critical flaw sizes and leakage flaw sizes for each postulated crack path in the DM weld and adjacent base material are determined and listed in Table 6-3. The calculated flaw size margins are 2 or higher (the required margin is 2).

It can be noted here that the PICEP leakage results are obtained at an outlet fluid temperature of 200°F. Generally, the sump temperature at which the fluid that leaked from the pipe is collected is lower. Hence, the amount of water collected at the sump has to be multiplied by the ratio of the density of the water at sump temperature to the density of water at 200°F. Typically, the sump water is at 120°F. Therefore, to obtain 2.0 gpm of leakage at the sump, one has to get a leak rate of 2.0*(8.249/8.037) = 2.053 GPM from the pipe. Compared to the leakage results reported in Table 6-1, this difference is small and is therefore not considered for reporting the results in Tables 6-1 and 6-2.

6.4 Leakage Comparison to the Original LBB Evaluation

A test case is also run to check the compatibility of the current methodology in this report with respect to the one in the leakage flaw size evaluation from the original LBB report [1]. The parameters used for the test case ('B'), such as geometry, material properties, and loads are given in Section 2.

A relative roughness of [redacted] is used [1, Section 5.2.2] per the original leakage evaluation. In the original report, no Ramberg-Osgood parameters are provided for the leakage analysis. Therefore, it is conservatively assumed that the plastic crack opening is negligible, which is ensured in the PICEP input file by using $\alpha = 0.0001$ and $n = 1$. Also, the following parameters are not provided in the original LBB report, and therefore, the PICEP defaults are assumed:

- Crack area at exit/Crack area at inlet (PICEP default = 1.0)
- Number of IGSCC 90 degree turns (PICEP default = 0)
- Number of IGSCC 45 degree turns (PICEP default = 0)
- Entrance Loss Coefficient C_d (PICEP default = 0.61)
- Friction factor (PICEP default = 0)

The results in Table 6-4 show that the leakage flaw size values are comparable. In addition to the relative roughness of [redacted] prescribed in Reference 1, the PICEP default roughness of 0.000197 inches [24] was used in the test case. The results in Table 6-4 show that the values are still comparable. The leakage crack size using PICEP is slightly higher (slightly less leakage for a given crack size) than the original LBB evaluation and, is therefore, conservative. The discrepancy in the results may be due to some of the crack morphology parameters assumed in the PICEP run.

Table 6-1. Leakage Flaw Size for 2 gpm Leakage Rate

Crack Location	DMW (in)		SSW (in)	
	Min. WOL Thickness	Max. WOL Thickness	Min. WOL Thickness	Max. WOL Thickness
1	5.93	6.35	4.88	5.41
2	5.39	5.89	5.04	5.54
3	9.97	10.03	4.74	5.25
4	5.17	5.72	4.74	5.25

Table 6-2. Leakage Rate for Leakage Flaw Size Equal to Half Critical Flaw Size

Crack Location	DMW (gpm)		SSW (gpm)	
	Min. WOL Thickness	Max. WOL Thickness	Min. WOL Thickness	Max. WOL Thickness
1	7.37	8.22	16.29	15.74
2	10.26	10.73	10.93	11.34
3	2.57	2.59	10.74	11.33
4	16.26	15.67	10.74	11.33

Table 6-3. Margin on Flaw Size

Crack Location	DMW (gpm)		SSW (gpm)	
	Min. WOL Thickness	Max. WOL Thickness	Min. WOL Thickness	Max. WOL Thickness
1	3.00	3.07	3.77	3.68
2	3.29	3.30	3.38	3.38
3	2.17	2.18	3.39	3.40
4	3.74	3.65	3.39	3.40

Table 6-4. Leakage Flaw Size Comparison for 2 gpm Leakage Rate

Leakage Flaw size for 10.75 inches (nominal OD)				
Axial Force (lbs)	Moment (in-lb)	Reference 6[1]	PICEP	Flaw-Size Ratio[2]
[redacted]			3.63[4] (3.55)[3]	1.10[4] (1.08)[3]

Notes:

(1) Reference 6 indicates the original Westinghouse LBB report

(2) $Ratio = \dfrac{RESULT_{PICEP}}{RESULT_{REF.1}}$

(3) PICEP roughness default of 0.000197 inches is used

(4) Relative roughness of [redacted] from the original Westinghouse LBB report is used

7.0 CONCLUSIONS

The effects of applying weld overlay repairs on the DM weld of the Unit 2 pressurizer surge line nozzle for the Prairie Island Nuclear Generating Plant along with the power uprate conditions on the LBB evaluation have been evaluated. It was observed that the application of the weld overlay results in residual stresses that are significantly reduced or at the inside surface and in the inner portion of the dissimilar metal weld. These stresses mitigate the effects of PWSCC in the Alloy 82/182 dissimilar metal weld. Furthermore, the use of highly resistant Alloy 52M weld metal, combined with improved inspection capability, provides additional assurance that through-wall cracks cannot occur at the DM weld locations. Crack growth evaluations were performed in Reference 6 to indicate that combined PWSCC and fatigue crack growth for axial and circumferential postulated flaws is within acceptable limits for a [redacted] operating interval.

The current evaluation was conducted using LBB assumptions similar to that used in the original Westinghouse evaluation, modified to account for the addition of the weld overlays and PU conditions. This evaluation demonstrates that with the application of the weld overlay, the LBB margins required in SRP 3.6.3 and NUREG-1061, Volume 3 and the requirements of GDC-4 are maintained for all postulated flaws. The effect of the application of the weld overlay is to increase the critical flaw size, resulting in additional margin between the critical flaw size and the leakage flaw size, even though leakage tends to be reduced due to the longer flow path and considerations of crack morphology for the Alloy 82/182 weld location.

Critical flaw sizes and leakage calculations were benchmarked against the original Westinghouse analyses. The current analysis is conservative for both the critical flaw size and leakage flaw size compared to the original LBB evaluations. A range of weld overlay thicknesses was also evaluated, showing that the actual thickness attained during overlay application does not change the LBB behavior significantly.

8.0 REFERENCES

[redacted]

2. a. NUREG-0800, "U.S. Nuclear Regulatory Commission Standard Review Plan, Office of Nuclear Reactor Regulation, Section 3.6.3, Leak-Before-Break Evaluation Procedure," March 1987.

   b. NUREG-0800, "U.S. Nuclear Regulatory Commission Standard Review Plan, Office of Nuclear Reactor Regulation, Section 3.6.3, Leak-Before-Break Evaluation Procedure," Revision 1, March 2007.

3. NUREG-1061, Volume 3, "Report of the U.S. Nuclear Regulatory Commission Piping Review Committee," prepared by the Piping Review Committee, NRC, April 1985.

4. [DIT, "PI U2 PRZ WOL Sizing Calculation- Surge Nozzle," NMC Document No. 32-9036640, Rev. 1][2].

[redacted]

[redacted]

7. ASME Boiler and Pressure Vessel Code, Section XI, 2001 Edition with Addenda through 2003.

8. Materials Reliability Program: Technical Basis for Preemptive Weld Overlays for Alloy 82/182 Butt Welds in PWRs (MRP-169), Rev. 1, EPRI, Palo Alto, CA: 2008. 1016602.

9. ASME Section XI Task Group for Piping Flaw Evaluation, ASME Code, "Evaluation of Flaws in Austenitic Steel Piping," Journal of Pressure Vessel Technology, Vol. 108, August 1986, pp. 352-366.

10. ASME Code Case N-504-3, "Alternative Rules for Repair of Classes 1, 2, and 3 Austenitic Stainless Steel Piping," Section XI, Division 1.

11. ASME Code Case N-740-2, "Dissimilar Metal Weld Overlay for Repair or Mitigation of Class 1, 2, and 3 Items," Section XI, Division 1.

12. EPRI NP-7103-D, "Justification for Extended Weld Overlay Design Life," Topical Report, January 1991.

13. EPRI NP-5881-LD, "Assessment of Remedies for Degraded Piping," June 1988.

14. DIT, "Leak before Break Evaluations (LBB) and Analysis including Licensing Submittal," Xcel Energy Document No. 1006-1.

15. DIT, "LBB Evaluations and Performing Associated Supporting Analysis," Xcel Energy Document No. 1006-4.

[redacted]

17. PINGP Surveillance Procedure SP 1173 [2173], *Stress Cycle Record*, Revision 31.

18. "XCEL Energy Prairie Island Unit 1 and 2 Transmittal of Xcel Requested Information to be provided to Structural Integrity Associates in Association with LBB Analysis," Westinghouse Letter NSP-09-90.

19. ASME Boiler and Pressure Vessel Code, Section II, *Material Properties*, 2001 Edition with Addenda through 2003.

20. ASME Boiler and Pressure Vessel Code, Section XI, 2001 Edition with Addenda through 2003.

21. Wilkowski, G, et.al, "Determination of the Elastic-Plastic Fracture Mechanics Z-factor for alloy 82/182 Weld Metal Flaws for Use in the ASME Section XI Appendix C Flaw Evaluation Procedures," Proceedings of ASME-PVP 2007.

22. Cofie, N.G., Miessi, G.A., and Deardorff, A.F., "Stress-Strain Parameters in Elastic-Plastic Fracture Mechanics," Transactions of the 10th International Conference on Structural Mechanics in Reactor Technology, Volume L – Inelastic Behavior of Metals and Constitutive Laws of Materials, August 14-18, 1989, Anaheim, Ca, USA, pp 91-96.

23. D. M. Norris and B. Chexal, "PICEP: Pipe Crack Evaluation Program (Revision 1)," EPRI NP-3596-SR, Revision 1, December 1987.

24. D. Abdollahian and B. Chexal, "Calculation of Leak Rates Through Cracks in Pipes and Tubes," EPRI NP-3395, Electric Power Research Institute, Palo Alto, CA, December 1983.

25. Wilkowski, G., Wolterman, R., and Rudland, D., "Impact of PWSCC and Current Leak Detection on Leak-Before-Break Acceptance," Proceedings of ASME Pressure Vessels and Piping Division Conference, Denver, CO, July 17 to July 21, 2005.

26. U.S. Nuclear Regulatory Commission, 10CFR50.55a.

27. DIT, " Prairie Island Unit 2 Pressurizer Surge Nozzle Weld Overlay Residual Stress Analysis," NMC Document No. 32-9067274, Rev. 0.

28. Performance Demonstration Initiative (PDI) Program Description, Rev. 2, Oct. 1, 2000.

29. NUREG-0313, "Technical Report on Material Selection and Processing Guidelines for BWR Coolant Pressure Boundary Piping," Revision 2, January 1988.

30. Materials Reliability Program: Primary Systems Piping Butt Weld Inspection and Evaluation Guidelines (MRP-139), EPRI, Palo Alto, CA: 2005. 1010087.

31. Email from Koehler, Christopher of Xcel Energy to Art McSherry of SIA, sent on Nov. 23, 2009, "PINGP PZR SWOL as-built thickness data," SI File No. 0900634.209.

APPENDIX A

CRITICAL FLAW SIZE EVALUATION METHODOLOGY

A.1 INTRODUCTION

Appendix C of Section XI of the ASME Code [A-1] has a method for evaluating flawed piping using net section collapse limit load methods. The methodology is based on a single material thin cylinder and can be used to determine the critical through-wall flaw size for an overlaid pipe. A modified approach is developed herein based on similar limit load methods, but has some additional considerations.

A.2 TECHNICAL APPROACH

A.2.1 Net Section Collapse Model for Cracked Pipe with Weld Overlays

Standard Review Plan (SRP) 3.6.3 [A-1] provides methods for determining critical flaw size using net section collapse model. The original methodology, as described in Reference 1, is based on a single material cylinder. In the present case, the original weld is repaired by applying a weld overlay using a different material compared to the original weld material. Hence, a revised methodology is needed to consider both the materials such that the intent of SRP 3.6.3 can be met.

Deardorff, A, et al. proposed a method [A-2] to determine the critical through-wall flaw size for circumferential cracked pipe with weld overlays. It is based on a net section collapse solution, but has some additional considerations due to the weld overlay:

- The effects of two materials are considered. The limit load tensile force and bending moment can be evaluated for the circumferential cracked pipe with weld overlays.
- The analytical model allows for the arbitrary definition of the circumferential through-wall crack length for the weld overlay, while both circumferential crack length and depth (in the radial direction from the inside wall) for the base material.
- The evaluation method allows for a reduction in the fracture toughness to be considered. The Z-factor for the reduced toughness material (e.g., thermal aged material) can be applied to the

specific material.

A.2.2 Methodology

Figure A-1 shows a sketch of the cross section of a cracked pipe with weld overlay. The notations in the figure are defined as follows:

α = half through-wall (TW) crack angle in weld overlay
β = half TW crack angle in original pipe (can be different than α)
γ = neutral axis angle
r_a = mean radius of weld overlay
r_b = mean radius of the uncracked material of the original pipe
r_c = mean radius of the original pipe
r_d = mean radius of the cracked material of the original pipe
r_i = inside radius of original pipe
t_a = thickness of weld overlay
t_b = thickness of the uncracked material the original pipe
t_c = thickness of original pipe
t_d = thickness of the cracked material of the original pipe ($t_c - t_b$)

The axial force equilibrium of can be expressed as:

$$R = \int_{\alpha}^{\pi-\gamma} A d\theta - \int_{\pi-\gamma}^{\pi} A d\theta + \int_{\beta}^{\pi-\gamma} B d\theta - \int_{\pi-\gamma}^{\pi} C d\theta$$

where,

R = half of the axial load
A = $\sigma_{fa}\, r_a\, t_a$
B = $\sigma_{fb}\, r_b\, t_b$
C = $\sigma_{fb}\, r_c\, t_c$

σ_{fa} = flow stress of weld overlay

σ_{fb} = flow stress of original pipe

Therefore, the neutral angle γ is given by:

$$\gamma = \frac{(A+B)\pi - \alpha A - \beta B - R}{2A+B+C} \quad (1)$$

Employing moment equilibrium, the plastic collapse moment can be expressed as:

$$M_b = \int_{\alpha}^{\pi-\gamma} A'\cos\theta d\theta - \int_{\pi-\gamma}^{\pi} A'(-\cos\theta)d\theta + \int_{\beta}^{\pi-\gamma} B'\cos\theta d\theta - \int_{\pi-\gamma}^{\pi} C'(-\cos\theta)d\theta$$

where,

M_b = half of the plastic collapse bending moment

A' = $Ar_a = \sigma_{fa} r_a^2 t_a$

B' = $Br_b = \sigma_{fb} r_b^2 t_b$

C' = $Cr_c = \sigma_{fb} r_c^2 t_c$

The remote bending stress in the uncracked pipe, based on shell theory is:

$$P'_b = \frac{2M_b}{\pi r_c^2 t_c} \quad (2)$$

As defined in ASME Code [A-3], the failure bending stress is defined as

$P'_b = SF(P_m + P_b) - P_m$ for high toughness material

$P'_b = Z(SF)(P_m + P_b + P_e / SF) - P_m$ for low toughness material

where,

P_e = primary membrane stress

P_b = primary bending stress

P_e = thermal expansion bending stress

SF = safety factor

Z = Z-factor for correcting for low toughness material

In the weld overlay process, the overlay material is usually Alloy 690 (52M) deposited using GTAW. Hence, the Z-factor only applies to the base material. Equation 5 of Reference 2 describes how the plastic collapse bending stress may be calculated for a two layer configuration as follows:

$$P'_b = (1 - M^*)[SF(P_m + P_b) - P_m] + M^*[Z(SF)(P_m + P_b + P_e / SF) - P_m] \quad (3)$$

where,

M^* = ratio of tension region material axial load due to underlying material by total axial load for tensile material

Note that in the above expression, M* is determined based on the axial load ratio, not the moment ratio as in Reference 2. Experience shows that use of the moment ratio could result in unrealistic M* values that are greater than 1.0 or less than zero due to the fact that the moment contribution due to material below the neutral axis can be negative.

With this approach, if it is assumed that the entire underlying material is cracked above the neutral axis, then $M^* = 0$ and the equation collapses back to the form for high toughness material. If there is no overlay material, then $M^* = 1.0$, and the equation becomes that for a low-toughness material where the complete effect of the thermal expansion moment must be included in the evaluation.

Substituting the neutral axis angle in Equation (1) into Equation (2), Equation (2) and Equation (3) can be solved and the critical circumferential flaw length for fixed crack depth in the base material can be obtained.

A.3 REFERENCES

A-1. U.S. Nuclear Regulatory Commission, Standard Review Plan 3.6.3, "Leak-before-Break Evaluation Procedures," Revision 1, March, 2007.

A-2. Deardorff, A. F., Cofie, N. G., Dijamco D. G. and Chintapalli A., "Net Section Plastic Collapse Analysis of Two-Layered Materials and Application to Weld Overlay Design," PVP2006-ICPVT11-93454, ASME PVP Conference 2006.

A-3. ASME Boiler and Pressure Vessel Code, Section XI, Rules for Inservice Inspection of Nuclear Power Plant Components (various Editions and Addenda).

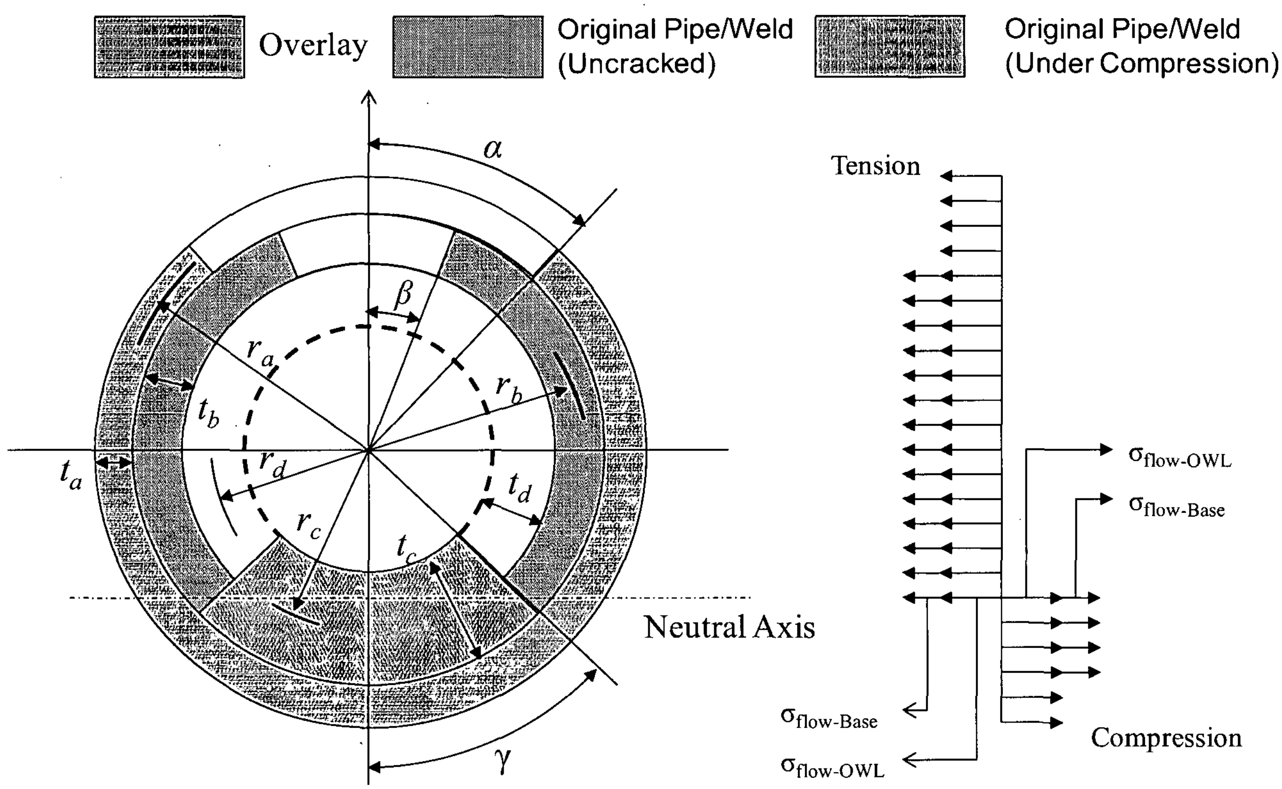

Figure A-1. Schematic of a Circumferentially Cracked Section with Weld Overlay

APPENDIX B

LEAKAGE EVALUATION METHODOLOGY

B.1 LBB METHODOLOGY

Leak-before-break evaluations require that leakage be calculated for the loads in piping systems expected to be used during normal plant operation. This typically includes the loads due to pressure in the piping and due to moments and axial forces resulting from dead weight and thermal expansion of the piping system.

In the original LBB evaluations for most plants, the leakage was calculated based on fatigue crack morphology, where the crack surface was expected to be quite smooth. Based on the occurrence of PWSCC in PWR piping systems, the potential existence of PWSCC cracking must be considered where the cracking could occur in susceptible materials. This is considered in the cases where a non-susceptible weld overlay is installed on a susceptible Alloy 82/180 weldment.

B.2 MORPHOLOGY EFFECTS ON LEAKAGE EVALUATION

Battelle Columbus and Engineering Mechanics Corporation of Columbus (EMC^2) have conducted research to assess the technology used in determining leakage through cracked piping with SCC morphology [B-1, B-2, B-3]. It has been determined that the crack morphology, characterized by the local roughness, number of flow path turns, and total leakage path length, is significantly different between fatigue cracking and SCC. For fatigue cracks, the flow path is relatively smooth and straight, whereas for SCC, the flow path is relatively rough and consists of many turns. A procedure has been proposed in NUREG/CR-6300 [B-2] that defines the surface roughness, effective flow path length and number of flow path turns as a function of the ratio of the crack opening displacement (COD, δ) to the global roughness (μ_G) of the flow path. For very tight cracks, there is a relatively longer flow path with many local turns, but the local roughness is relatively lower. For cracks with a much larger opening, the roughness is better represented by the global roughness but the number of turns and effective flow path length decrease. Although not confirmed by testing or detailed fluid mechanics analysis, this model is a reasonable representation of the morphology effects due to SCC on leakage flow.

For defining the crack morphology, the model proposed by Battelle is considered that take into account both global roughness μ_G and the local roughness μ_L as illustrated in Figure B-2 [B-1].

These are then combined with δ, the COD, by the following set of equations to develop an effective roughness μ.

$$\mu = \begin{cases} \mu_L, & 0.0 \le \dfrac{\delta}{\mu_G} < 0.1 \\ \mu_L + \dfrac{\mu_G - \mu_L}{9.9}\left[\dfrac{\delta}{\mu_G} - 0.1\right], & 0.1 \le \dfrac{\delta}{\mu_G} \le 10 \\ \mu_G, & \dfrac{\delta}{\mu_G} > 10 \end{cases} \qquad \text{(B-1)}$$

A similar set of equations were developed to determine the effective number of turns (NT), with the assumption that the number of turns decreases to about 0.1 of the local number of turns, (NL) when the crack opening displacement is equal to 10 times or more of the global roughness.

$$n_t = \begin{cases} n_{tL}, & 0.0 \le \dfrac{\delta}{\mu_G} < 0.1 \\ n_{tL} - \dfrac{n_{tL}}{11}\left[\dfrac{\delta}{\mu_G} - 0.1\right], & 0.1 \le \dfrac{\delta}{\mu_G} \le 10 \\ 0.1 n_{tL}, & \dfrac{\delta}{\mu_G} > 10 \end{cases} \qquad \text{(B-2)}$$

Similarly, the total flow path length is increased due to the crack being skewed relative to the pipe wall and due to the turns within the material, as shown in Figures B-1 and B-2. Then, the ratio between the total flow path length L_a and the pipe wall thickness t is determined by:

$$\frac{L_a}{t} = \begin{cases} K_{G+L}, & 0.0 \le \dfrac{\delta}{\mu_G} < 0.1 \\ K_{G+L} - \dfrac{K_{G+L}-K_G}{9.9}\left[\dfrac{\delta}{\mu_G}-0.1\right], & 0.1 \le \dfrac{\delta}{\mu_G} \le 10 \\ K_G, & \dfrac{\delta}{\mu_G} > 10 \end{cases} \qquad \text{(B-3)}$$

The EPRI-developed computer program PICEP [B-4] is not designed to directly include the methods for computing morphology using the interpolation method proposed in NUREG/CR-6300. To determine the effects of crack morphology on leakage flaw sizes, additional calculations can be conducted using PICEP with input revised to simulate SCC morphology.

It is further observed that the method used in PICEP for addressing the effects of number of turns is not consistent with the approach used in the NRC-sponsored SQUIRT computer program developed by Battelle for computation of leakage through pipes and tubes [B-5]. In PICEP, the number of turns has been determined (by performing a number of different analyses) to be simulated by adding an equivalent L/D=26 for 45-degree turns and L/D=50 for 90-degree turns. These equivalent additional lengths are appropriate for use in determining the pressure drop through typical piping components. However, when the roughness (ε) is increased to be large comparable to the hydraulic diameter (D_H), the effect of the number of turns is further amplified since it is multiplied by an increased friction factor (f). In SQUIRT, a more fundamental approach is used for the number of turns in that it is recommended that a turn be equivalent to the loss of one velocity head, without the additional multiplying factor of increased roughness.

To determine input to PICEP to simulate a crack with both fatigue and PWSCC morphology in the same crack, an equivalent number of turns and equivalent roughness are determined.

The method is based on the fact that the flow resistance along a flow path is made up of the friction resistance and the discontinuity (e.g., turns) resistance. The pressure differential is determined by multiplying the sum of the friction (fL/D) and discontinuity (K) loss factors by the velocity pressure in the flow path.

In PICEP the turns and friction resistance are lumped together.

Loss Factor = $f\,(t/D_h + 50N_{90})$ for 90 degree turns

= $f\,(t/D_h + 26N_{45})$ for 45 degree turns

where

f	=	friction factor
	=	$(2\log(D_H/2\,\varepsilon) + 1.74)^{-2}$ [B-4]
ε	=	roughness (defined as μ by Battelle)
t	=	pipe wall thickness
N_{90}, N_{45}	=	number of 90-degree or 45-degree turns in leak path
D_h	=	hydraulic diameter = $4\,A/W_p$
A	=	flow path cross-section area
W_p	=	wetted perimeter of flow path cross-section area.

($D_h = \pi/2$ COD for an elliptical crack where COD is the center point crack opening displacement)

For flow through a complex crack consisting of a cracked weld followed by a cracked overlay, there will similarly be losses due to friction and turns. To simulate this in PICEP, an equivalent friction factor must be determined that will yield the same friction as for the complex crack case.

$$f_{eq}(t/D_h) = \Sigma\, f_i\,(L_{ai}/D_h)$$

where

f_i = friction factor for the revised roughness for each crack face

L_{ai} = revised flow path length for each crack face

For input to PICEP, the equation above for the friction factor can be used to solve for an equivalent roughness that will produce the correct loss factor.

The equivalent number of turns can be similarly determined.

$$f\,(50N_{90}) = \Sigma\, N'_i\, L_{ai}\, K_{90}$$

where

N'_I = number of 90-degree turns per unit flow path length for each crack face

K_{90} = loss coefficient (number of velocity heads) for each 90-degree turn

Thus, the number of turns to be used in a PICEP analysis can be determined by:

$$N_{PICEP\text{-}90} = 0.02\ (\Sigma\, N'_i\, L_{ai}\, K_{90})/\ f_{eq}$$

where

N' = number of 90° turns per inch predicted for a specific crack morphology

L = total flow path length = t x K_{G+L} (from EQ. B-3)

Similarly, the number of 45-degree turns to input in a PICEP run can be determined as:

$$N_{PICEP\text{-}45} = N_{PICEP\text{-}90} \times 50/26$$

B.3 METHOD FOR EVALUATION USING PICEP

1. A baseline PICEP case is run using the default values for roughness (e.g., 0.000197 inches for fatigue cracks) [B-6] and no turns to simulate fatigue cracking. This run will produce up to twenty leakage calculations for increasing crack size, and report the corresponding COD for each case. (This run reads information from a special text input file that was created for a previous PICEP pre-process called RUNPICEP, which was created to ease the creation of input to PICEP – as opposed to the "card" style of input currently required.)

2. For each of the leakage calculations above, the modified parameters to reflect combined fatigue/SCC morphology are calculated, since the modified morphology parameters (number of turns, deviation from straightness and roughness) are functions of COD. The roughness and number of equivalent 45-degree or 90-degree turns to use in PICEP can be calculated using the equations above. Since PICEP accepts only an integer number of turns, the number of 45-degree turns or 90-degree turns that most nearly simulates the total fluid resistance is used. A series of PICEP runs are then made with the revised morphology parameters, with each run being conducted for only the single crack length. The results for all crack sizes are reported in a single output file.

3. The crack size for any specific leakage rate can be determined by interpolation from the modified computer output.

B.4 REFERENCES

B-1. "Probabilistic Pipe Fracture Evaluations for Leak-Rate Detection Applications," NUREG/CR-6004, U.S. Nuclear Regulation Commission, April 1995.

B-2. NUREG/CR-6300, "Refinement and Evaluation of Crack-Opening Analyses for Short Circumferential Through-Wall Cracks in Pipes," U.S. Nuclear Regulation Commission, April 1995

B-3. D. Ruland, R. Wolterman, G. Wilkowski, R. Tregoning, "Impact of PWSCC and Current Leak Detection on Leak-Before-Break," Proceedings of Conference on Vessel Head Penetration, Inspection, Cracking, and Repairs, Sponsored by USNRC, Marriot Washingtonian Center, Gaithersburg, MD, September 29 to October 2, 2003.

B-4. D. M. Norris and B. Chexal, "PICEP: Pipe Crack Evaluation Program (Revision 1)," EPRI NP-3596-SR, Revision 1, December 1987.

B-5. SQUIRT (Seepage Quantification of Upsets In Reactor Tubes) User's Manual, Windows Version 1.1, March 24, 2003, Battelle, Columbus, OH.

B-6. D. Abdollahian and B. Chexal, "Calculation of Leak Rates Through Cracks in Pipes and Tubes," EPRI NP-3395, Electric Power Research Institute, Palo Alto, CA, December 1983.

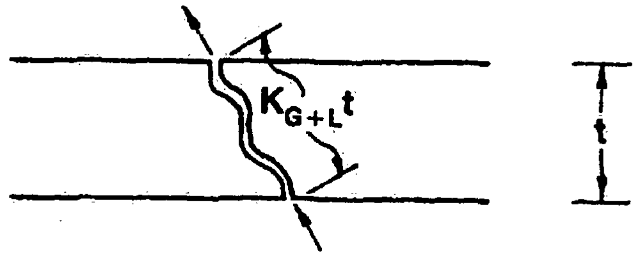

Small COD

Figure B-1. Flow Path Deviation As Affected by Roughness and Crack Opening Displacement

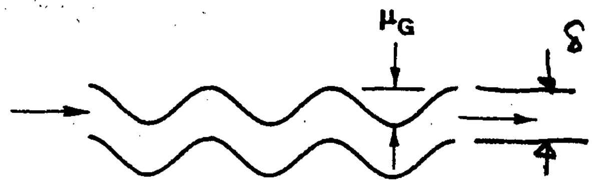

Large COD

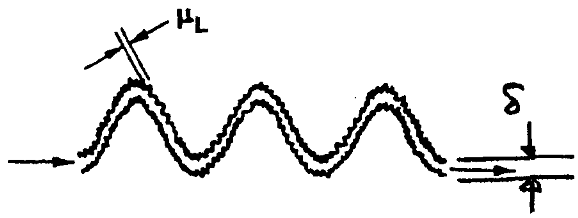

Small COD

Figure B-2. Roughness Depiction for Small and Large Crack Opening Displacements

APPENDIX C

DETERMINATION OF RAMBERG-OSGOOD PARAMETERS

C.1 INTRODUCTION

The Ramberg-Osgood (R-O) stress-strain parameters (α and n) are required for elastic-plastic fracture mechanics analysis involving critical flaw size and leakage determination. These parameters may be a function of temperature. This appendix provides the methodology for determining the R-O parameters from basic mechanical properties determined from the ASME Code. It also includes a method of making adjustments to the R-O parameters at a different temperature when the R-O parameters at another temperature are known.

C.2 METHODOLOGY

The Ramberg-Osgood model is in the form:

$$\frac{\varepsilon}{\varepsilon_0} = \frac{\sigma}{\sigma_0} + \alpha\left[\frac{\sigma}{\sigma_0}\right]^n \qquad \text{(C-1)}$$

Where σ and ε are the true stress and true strain, σ_o and ε_o are the reference stress and reference strain (in general yield stress and yield strain) and α and n are the Ramberg-Osgood (R-O) parameters.

When the stress-strain curve at the temperature of interest is available, the R-O parameters can be obtained by curve fitting over the strain range of interest. In the absence of the stress-strain curve of the material, a methodology for determining the R-O parameters based on ASME Code-specified mechanical properties has been provided in Ref. C-1. The suggested method is described by the following equations:

$$\alpha \approx \frac{0.002}{e_y} \qquad \text{(C-2)}$$

$$n = \frac{\ell n\left[\frac{1}{\alpha}\left(\frac{\ell n(1+e_u)}{\ell n(1+e_y)} - \frac{S_u(1+e_u)}{S_y(1+e_y)}\right)\right]}{\ell n\left[\frac{S_u(1+e_u)}{S_y(1+e_y)}\right]} \quad \text{(C-3)}$$

where S_u and S_y represent ultimate stress and yield stress respectively. They can be obtained from the ASME Code[C-2] for a wide range of temperatures. The yield strain (e_y) is determined as:

$$e_y = \frac{S_y}{E} \quad \text{(C-4)}$$

where E (modulus of elasticity) can also be obtained from the ASME Code. The ultimate strain (e_u) is not specified at all temperatures in the ASME Code, hence the room temperature minimum elongation value specified in the ASME Code, Section II [C-2] is assumed for all temperatures. The methodology in any case is not sensitive to the choice of e_u [C-1] when determining α and n by using equation (C-2) and (C-3).

C.3 REFERENCES

C-1 Cofie, N.G., Miessi, G.A., and Deardorff, A.F., "Stress-Strain Parameters in Elastic-Plastic Fracture Mechanics," Transactions of the 10th International Conference on Structural Mechanics in Reactor Technology, Volume L – Inelastic Behavior of Metals and Constitutive Laws of Materials, August 14-18, 1989, Anaheim, Ca, USA, pp 91-96.

C-2 ASME Boiler and Pressure Vessel Code, Section II 2001 Edition with 2003 Addenda.